Excess Gibbs free energy models for studying ionic liquid-H_2O binary system

Chunyan Ma,[a,*] Yanxin Wang,[b] Yunhao Sun,[a] Xiaohua Lu,[b] and Xiaoyan Ji[a,*]

[a] *Division of Energy Science/Energy Engineering, Department of Engineering Science and Mathematics, Luleå University of Technology, Luleå, 971 87, Sweden*

[b] *State Key Laboratory of Material-Oriented Chemical Engineering, Nanjing Tech University, Nanjing, 210009, P. R. China*

E-mails: chunyan.ma@ltu.se, xiaoyan.ji@ltu.se

Abstract

In this work, the excess Gibbs free energy models, *i.e.*, non-random two-liquid (NRTL) model, electrolyte NRTL model, and electrolyte NRTL model including new strategies (association or hydration), were used to describe the macroscale properties and interpret the microstructure, clarifying the role of association and hydration in model development, and the enthalpy of mixing of three imidazolium-based IL-H_2O systems containing the same cation but different sizes of anions, *i.e.*, Cl^-, Br^-, and I^- were measured for the first time to provide systematic data for model development. The models were developed and evaluated based on the newly measured data and the osmotic coefficient from the literature. The model reflecting the intrinsic mechanism of dissociation and hydration competition gives the best modeling results. The real ionic strength predicted from the identified model was quantitatively correlated with the electrical conductivities.

Keywords: Models, ionic liquid, enthalpy of mixing, association, hydration

1. Introduction

Recently, ionic liquids (ILs) have been regarded as promising candidates to replace the toxic organic solvents because of their outstanding properties, *i.e.*, negligible vapor pressure, good thermal and chemical stability, and designable feature.[1] It has been suggested that ILs will revolutionize the process industry in the coming years, and much research has been carried out in various areas, for example, CO_2 capture and separation,[2] lubrication and tribology,[3] biomass dissolution,[4] and catalysis[5]. Although IL-based technologies are promising in various applications, their viscosities are often relatively high, being impractical in many industrial applications. There are numerous reports that the addition of small amounts of water into ILs can largely eliminate the drawbacks of high viscosity.[6-9] For instance, Fendt *et al*.[6] investigated the viscosities of acetate- or chloride-based ILs by adding water and some other co-solvent. It showed that a small amount of water (mass fraction of 10 %) reduced the viscosity to almost 50% that of the neat IL. In fact, many ILs are strongly hygroscopic so that small traces of water absorbed from the atmosphere cannot be avoided.[10] Torrecilla *et al*.[10] studied the effect of the relative humidity of air on the physical properties (*e.g.*, density, viscosity) of imidazolium-based IL. The results indicated that the small trace of water from the atmosphere affected the microstructure of IL, leading to a noticeable change in the physical properties. Water is often involved in the process either as an impurity or an important co-solvent.[11] As reported by Ma *et al*.[12], the addition of water reduced the viscosity of N-alkyl-N-methylmorpholinium-based ILs, giving rise to a reduced energy demand and equipment size for CO_2 separation from biogas. All in all, the addition of H_2O can be a preferable option to tackle the obstacles of IL-based technologies for practical applications such as gas separation. It is, therefore, crucial to study IL-

H_2O systems, especially to quantitatively describe their properties in the whole composition range with theoretical models.

Modeling thermodynamic properties of IL-H_2O binary systems based on thermodynamic models, such as the non-random two-liquid model (NRTL), is a pathway to quantitatively describe the properties. Because of the complexity of these systems, until now, it is still a challenge to describe the properties and phase equilibria of IL-H_2O binary systems. Thermodynamic models developed to date to describe IL-H_2O binary systems are minimal, and most of them are for aqueous IL solutions, *i.e.*, from infinitely dilute IL to a certain low concentration of IL. Besides, most of the models are primarily based on the equation of state (EOS). For example, Li *et at*.[13] modeled the properties of the aqueous solution of nine imidazolium-based ILs based on an equation of state of square-well chain fluid with variable range (SWCF-VR). In modeling, it was assumed that the IL was partially dissociated into cations and anions, and therefore, the cations, anions, and neutral IL molecules coexist in the solution. However, this model was only studied for aqueous IL rather than IL-concentrated solution. In work reported by Mahato *et al*.[14] and Tsioptsias *et al*.[15], IL was modeled as a molecule without ionic interaction, and the model was developed based on a narrow compositional range. The modeling based on a wide compositional range is scarce. Besides EOS, the excess Gibbs free energy (G^E) model is widely used in the liquid phase. However, the work for IL-H_2O systems based on the G^E model is mostly molecule-based, *i.e*., IL is considered as a molecule. Only a few works based on the G^E model considered ions in IL-H_2O systems.[16,17] [18] Simoni et al.[17], for the first time applied an electrolyte G^E model to model liquid-liquid equilibria for mixtures that involve ILs by assuming complete dissociation of the IL. Li et al.[18] modeled the association of

three aqueous imidazolium-based IL systems with symmetric electrolyte NRTL model using vapor-liquid equilibrium (VLE) data.

In our previous work,[19] a comprehensive literature survey revealed that the competition of IL-dissociation and ion hydration is an important feature for the IL-H_2O system ranging from a pure IL to infinitely dilute IL solution,[19] and a conceptual framework incorporating dissociation and hydration was proposed for developing thermodynamic models. However, no model has been developed with such a concept, and it is still unclear how to develop such a model. Meanwhile, our literature survey also showed that owing to the large size of the cation, its hydration may be ignored, and the hydration of anion is dominated.[19] Especially, for the halide-based ILs, their strong hydration at the infinitely dilute solution depends on the type of halide ions. Modeling these IL-H_2O systems with different halide ions will be vital to reflect the role of association and hydration in model development.

The model development calls for reliable and systematic experimental data covering an entire compositional range. For the IL-H_2O systems with the halide-based IL, the osmotic coefficient has been widely measured but only available in an IL diluted solution due to the negligible vapor pressure of IL. The enthalpy of mixing directly reflects the nonideal behavior during the mixing process between IL and H_2O over the entire compositional range, which can be used as a desirable input to develop thermodynamic models.[16] However, the available data is very scarce, and most of them are within a narrow compositional range. Besides that, the electrical conductivity is another property that provides valuable information on ion-ion and ion-solvent interaction in solution.[20] Again, the experimental data of conductivity is usually available at low concentrations. The data over the entire compositional range have been minimally

measured and reported, and thus, systematic data covering the whole composition range needs to be determined.

In this work, three typical halide-based IL-H_2O systems with the same cation, *i.e.*, 1-hexyl-3-methylimidazolium but different sizes of anions, *i.e.*, chloride (Cl^-), bromide (Br^-), and iodide (I^-), were selected to carry out modeling. The models, including the non-random two liquid (NRTL) model, electrolyte NRTL (eNRTL) model, and eNRTL model including two new strategies, were studied from performance to microstructure interpretation in order to clarify the role of association and hydration. The enthalpy of mixing of these systems over the entire compositional range was measured and reported for the first time, and the measured data in this work, together with the available osmotic coefficient from the literature, were used as input in modeling these IL-H_2O systems. The performance of different models and strategies were compared and discussed. The microstructure (association degree, real ion strength, etc.) of these systems were further analyzed about the hydration number and ionic size effect with the new strategies. In addition, the electrical conductivity over the whole compositional range of these systems at different temperatures was also measured. The effects of water content, the size of anions, and temperature on the electrical conductivity were discussed based on experimental results. Besides, the relationship between electrical conductivity and real ion strength predicted from modeling was further analyzed.

2. Experimental Section

2.1 Chemicals. Three ILs, including 1-hexyl-3-methylimidazolium chloride (HmimCl), 1-hexyl-3-methylimidazolium bromide (HmimBr), and 1-hexyl-3-methylimidazolium iodide (HmimI), were purchased from Lanzhou Greenchem IL_S, LICP., CAS, China. High-quality deionized

water (conductivity, <0.055 μS·cm^{-1}) was used during the process. These ILs were dried in a vacuum oven for 24 h before use to avoid the trace of moisture.

2.2 Enthalpy of mixing (H_m). The molar enthalpy of mixing H_m was measured by the TAM Air isothermal microcalorimeter (TA Instruments, USA), and its operating temperature was controlled by air circulation. The temperature deviation is within 0.02 K. The parallel dual-chamber measurement channels, *i.e.*, the measurement channel and the reference channel, were used during the measurement. In the measurement channel, a precise amount of IL was placed in a 20 ml ampoule, while a precise amount of water was placed in a Hamilton syringe with automatic agitation on top of the ampoule. In the reference channel, the water and IL were premixed in the required ratio as the same as that in the measurement channel, which was used to eliminate the measurement error caused by the change of external temperature. The signal generated during the entire experiment was automatically recorded. When the system reached equilibrium, that is, the heat flow kept constant with time, the heat Q was determined by the area of the observed peaks on the baseline in each injection. All the measurements were repeated at least three times, and the average value was reported. The molar enthalpy of mixing H_m was calculated by the heat Q divided by the quantity of the IL and water involved in this system, as shown in Eq.).

$$H_m = -\frac{Q}{n_{IL} + n_{H_2O}} \quad (1)$$

where Q represents the heat recorded during each experiment; n_{IL} and n_{H2O} are the mole weights of IL and water, respectively.

2.3 Electrical conductivity. The electrical conductivity was measured by a Mettler Toledo conductivity meter (model FE38-Standard). The accuracy of conductivity measurements was calibrated beforehand by the standard buffer solutions with different conductivities, *i.e.*, 84, 1413, and 1.288 μS·cm^{-1}. The average uncertainty in the measurements was ± 0.05 mS·cm^{-1}. The temperature was controlled by an external water bath DK-S24. The LE703 electrode with a built-in temperature probe was used to measure the temperature. The uncertainty of the temperature of the conductivity cells was within ± 0.5 K. The IL-H_2O solutions were prepared by weighing with a digital analytical balance (Sartorius SECURA225D-1CN) with a precision of ±10^{-5} g. All IL-H_2O solutions were tightly sealed and stirred for more than 2 h to ensure thorough mixing, and then the measurements were carried out immediately. All the measurements were repeated three times, and the average value was reported.

3. Thermodynamic modeling

3.1 Excess Gibbs free energy (G^E) model. To consider the real behavior of the mixtures, an expression for the excess Gibbs free energy (G^E) in such mixtures is needed. Two G^E models, that is, the NRTL model and eNRTL model, were discussed in this work.

3.1.1 NRTL model. NRTL model is a molecule-based activity coefficient (γ) model reflecting the nonideal behavior of the binary or multicomponent systems.[21] In the NRTL model, G^E is only contributed from the short-range interaction. Therefore, the activity coefficient derived from G^E only contains the short-range interaction term, as shown in Eq. (2). In modeling, the ILs are assumed to be completely associated. In other words, each cation is completely paired with an anion, and thus each ion-pair is considered as a single molecular species in the solution.

$$G^{E} = RT\sum_{i}^{m} x_i \ln \gamma_i$$

$$\ln \gamma_i = \frac{\sum_{j=1}^{m} \tau_{ji} G_{ji} x_j}{\sum_{l=1}^{m} G_{li} x_l} + \sum_{j=1}^{m} \frac{G_{ij} x_j}{\sum_{l=1}^{m} G_{lj} x_l} \left[\tau_{ij} - \frac{\sum_{r=1}^{m} x_r \tau_{rj} G_{rj}}{\sum_{l=1}^{m} G_{lj} x_l} \right]$$

$$G_{ij} = \exp\left(-c_{ij}\tau_{ij}\right), \tau_{ij} = \Delta g_{ij}/RT = (g_{ij} - g_{jj})/RT, c_{ij} = c_{ji} (i \neq j) \quad (2)$$

where R is the ideal gas constant, 8.314 J·mol^{-1}·K^{-1}; T is temperature, K; x_i is the true mole fraction of component i; τ_{ij} is interaction parameters, which is related to the interaction energy parameters $\triangle g_{ij}$; c_{ij} is the nonrandomness factor; and m is the number of species.

3.1.2 eNRTL model. The eNRTL model was first proposed by Chen,[22], which combines the electrostatic (long-range interaction) contribution using the Pitzer's modification of Debye-Hückel (PDH) theory with the NRTL model. In applying the NRTL model to the short-range interaction contribution, two assumptions were introduced to elucidate the local composition of electrolyte solutions, that is, like-ion repulsion assumption and local electroneutrality assumption. Some work has applied eNRTL to the systems that involve ILs[16-18], where the symmetric reference state was suggested. In this work, the symmetric eNRTL model (pure fused salt as the reference state) was used for describing the $G^{E,}$ including two interaction contributions as shown in Eq. (3): a short-range interaction contribution ($G^{E,\,SR}$), a long-range electrostatic contribution ($G^{E,\,LR}$).

$$G^{E} = G^{E,\,SR} + G^{E,\,LR} \quad (3)$$

According to the eNRTL model proposed by Chen *et al*.[23], the excess Gibbs free energy from short-range interaction contribution $G^{E,\,SR}$ is expressed as eq. (4).

$$G^{E,SR}/RT = \sum_m x_m \frac{\sum_j^n x_j G_{jm}\tau_{jm}}{\sum_j^n x_j G_{jm}} + \sum_c x_c \sum_a \left(\frac{x_a}{\sum_{a'} x_{a'}}\right) \frac{\sum_j^n x_j G_{jc,ac}\tau_{jc,ac}}{\sum_j^n x_j G_{jc,ac}} + \sum_a x_a \sum_c \left(\frac{x_c}{\sum_{c'} x_{c'}}\right) \frac{\sum_j^n x_j G_{ja,ca}\tau_{ja,ca}}{\sum_j^n x_j G_{ja,ca}} \quad (4)$$

where $G_{jc,ac}$=exp(-$c_{jc,ac}\tau_{jc,ac}$); $G_{ja,ca}$=exp(-$c_{ja,ca}\tau_{ja,ca}$); $\tau_{jc,ac}=\Delta g_{jc,ac}/RT=(g_{jc}-g_{ac})/RT$; $\tau_{ja,ca}=\Delta g_{ja,ca}/RT=(g_{ja}-g_{ca})/RT$; j= *a, c, m*; $c_{jc,ac}$ and $c_{ja,ca}$ are the nonrandomness factor.

The excess Gibbs free energy from long-range interaction $G^{E,\,LR}$ is calculated by the PDH theory[24]**:**

$$G^{E,LR}/RT = -\left(4A_x I_x/\rho\right)\ln\left[\left(1+\rho I_x^{1/2}\right)\Big/\left(1+\rho\left(I_x^0\right)^{1/2}\right)\right]$$
$$A_x = \frac{1}{3}\left(\frac{1000}{M_s}\right)^{1/2}\left(2\pi N_A d_s\right)^{1/2}\left(\frac{Q_e^2}{4\pi\varepsilon_0 D_s k_b T}\right)^{3/2}$$
$$I_x = \frac{1}{2}\sum_i x_i z_i^2 \quad (5)$$

where A_x is the Debye–Hückel parameter; I_x is the ionic strength based on mole fraction; I_x^0 is the ionic strength for pure fused salt, which is ½ for singly charged ions; M_s is the molecular weight of the solvents, g·mol^{-1}; ρ is the closest approach parameter, 14.9; N_A is Avogadro's number, 6.02251×10^{23} mol^{-1}; d_s is the density of the solvent, kg·m^{-3}; Q_e is the electron charge, -1.602×10^{-19} C; D_s is the dielectric constant of the solvent; ε_0 is the permittivity of free space, 8.854×10^{-12} C^2·N^{-1}·m^{-2}; k_b is the Boltzmann constant, 1.38054×10^{-23} m^2·kg·s^{-2}·K^{-1}; and z_i is the charge number of species *i*.

For an uncharged species or molecular species, the activity coefficient is given by:

$$\ln \gamma_m = \ln \gamma_m^{SR} + \ln \gamma_m^{LR} \quad (6)$$

The contribution of short-range interactions to the activity coefficient was calculated by the expression in Eq. (7).[23,25]

$$\ln \gamma_m^{SR} = \frac{\sum_j \tau_{jm} G_{jm} x_j}{\sum_j G_{jm} x_j} + \sum_{m'} \frac{x_{m'} G_{mm'}}{\sum_j x_j G_{jm'}} \left[\tau_{mm'} - \frac{\sum_j x_j \tau_{jm'} G_{jm'}}{\sum_j x_j G_{jm'}} \right] + \sum_c \sum_a \frac{x_a}{\sum_{a'} x_{a'}} \frac{x_c G_{mc,ac}}{\sum_j x_j G_{jc,ac}} \left[\tau_{mc,ac} - \frac{\sum_j x_j \tau_{jc,ac} G_{jc,ac}}{\sum_j x_j G_{jc,ac}} \right] + \sum_a \sum_c \frac{x_c}{\sum_{c'} x_{c'}} \frac{x_a G_{ma,ca}}{\sum_j x_j G_{ja,ca}} \left[\tau_{ma,ca} - \frac{\sum_j x_j \tau_{ja,ca} G_{ja,ca}}{\sum_j x_j G_{ja,ca}} \right] \quad (7)$$

The contribution of long-range electrostatic force to the activity coefficient of uncharged species was calculated by Eq. (8) according to PDH theory.[24]

$$\ln \gamma_m^{LR} = 2 A_x I_x^{3/2} / \left(1 + \rho I_x^{1/2} \right) \quad (8)$$

The eNRTL model originally formulated by Chen *et al*.[23] operates under the assumption that all electrolyte components are completely dissociated in solution. Because the interaction energies are symmetric, it has been inferred that for a binary pair of single completely dissociated electrolyte and single solvent the binary interactions $\tau_{am}=\tau_{cm}=\tau_{ca,m}$ and $\tau_{mc,ac}=\tau_{ma.ca}=\tau_{m,ca}$.[22] It means that parameters $\tau_{ca,m}$ and $\tau_{m,ca}$ are the only two adjustable parameters.

3.2 New strategies. The mixing of IL with water results in a mixture of water molecules, IL ion-pair, and ions according to molecular simulation. The existence of association[26] and hydration have been proved by the mechanistic study. For the model, including long-range electrostatic

contribution, to describe the complicated interactions in these systems, two new strategies were proposed in this work.

3.2.1 Strategy 1: with hydration equilibrium but no association

In this strategy, an IL was dissociated into ions (C^+ and A^-), and no ion-pairs (CA) existed. According to the fundamental assumption of the eNRTL model that like-ion repulsion forces are extremely large, the local composition of a cation around a cation or anion around anion is zero. Due to a smaller size of anions, A^-, the ion-dipole forces between anion A^- and H_2O were remarkedly stronger than those between cation C^+ and H_2O, according to *MD/MC* simulation.[19] Therefore, the hydration of C^+ was neglected, while the hydration equilibrium of anion A^- was added, as shown by the reaction below:

$$A^- + h_w H_2O \overset{K_h}{\Leftrightarrow} A^- \cdot h_w H_2O \qquad (9)$$

where K_h is the hydration equilibrium constant, $\ln K_h = A_1 + A_2/T$; h_w is the numbers of water molecules in a hydration complex ($A^- \cdot h_w H_2O$).

The hydration equilibrium constant is described by:

$$K_h = \frac{a_{A^- \cdot h_w H_2O}}{a_{A^-} \cdot \left(a_{H_2O}\right)^{h_w}} = \frac{x_{A^- \cdot h_w H_2O}}{x_{A^-} \cdot \left(x_{H_2O}\right)^{h_w}} \cdot \frac{\gamma_{A^- \cdot h_w H_2O}}{\gamma_{A^-} \cdot \left(\gamma_{H_2O}\right)^{h_w}} \qquad (10)$$

where a, x, and γ are the true activity, true mole fraction, and true activity coefficient of different species, respectively.

Thus, in the IL-H_2O binary systems, there are four true species, *i.e.*, cations (C^+), anion (A^-), hydrated anion ($A^- \cdot h_w H_2O$) and H_2O. The following mass balance is based on the IL-H_2O binary

systems with N_{H2O} apparent moles of water and N_{CA} apparent moles of IL. The number of moles of free water ($n^{f}_{H_2O}$), free C^+ ($n^{f}_{C^+}$) and free A^- ($n^{f}_{A^-}$) is:

$$n^{f}_{H_2O} = N_{H_2O} - h_w \cdot n^{f}_{A^- \cdot h_w H_2O}$$
$$n^{f}_{C^+} = N_{CA};\ n^{f}_{A^-} = N_{CA} - n^{f}_{A^- \cdot h_w H_2O} \qquad (11\text{-}1)$$

where $n^{f}_{A^- \cdot h_w H_2O}$ are the number of moles of the hydrated anion ($A^- \cdot h_w H_2O$) in this system.

The total number of moles (n_T) in the solution is:

$$n_T = n^{f}_{H_2O} + n^{f}_{C^+} + n^{f}_{A^-} + n^{f}_{A^- \cdot h_w H_2O} = N_{H_2O} + 2N_{CA} - h_w \cdot n^{f}_{A^- \cdot h_w H_2O} \qquad (11\text{-}2)$$

Therefore, the true mole fractions of all species are given by:

$$x_{H_2O} = n^{f}_{H_2O} / n_T$$
$$x_{C^+} = n^{f}_{C^+} / n_T$$
$$x_{A^- \cdot h_w H_2O} = n^{f}_{A^- \cdot h_w H_2O} / n_T$$
$$x_{A^-} = 1 - x_{C^+} - x_{A^- \cdot h_w H_2O} - x_{H_2O} \qquad (11\text{-}3)$$

The hydration equilibrium represents the interaction between A^- and H_2O, and thus, the binary interaction between $A^- \cdot h_w H_2O$ and H_2O was neglected. As mentioned in the original eNRTL model, because the interaction energies are symmetric, it has been inferred that for a binary pair of single completely dissociated electrolyte and single solvent, the binary interactions $\tau_{am}=\tau_{cm}=\tau_{ca,m,}$ and $\tau_{mc,ac}=\tau_{ma.ca}=\tau_{m,ca}$.[22] Therefore, it remains three groups of adjustable parameters, including two binary interaction parameters $\tau_{ca,m}$, $\tau_{m,ca}$, and one hydration equilibrium constant K_h.

3.2.2 Strategy 2: with dissociation equilibrium and fully hydration

This strategy was made that cations C^+ exist as "free" species and anions A^- as complexes containing h_w water molecules (a hydration complex). The association or dissociation equilibrium in these systems is expressed in Eq. (12):

$$CA + h_w H_2O \overset{K_a}{\Leftrightarrow} C^+ + A^- \cdot h_w H_2O \qquad (12)$$

where K_a is the association equilibrium constant, and $\ln K_a = B_1 + B_2/T$.

The association equilibrium constant K_a is described by:

$$K_a = \frac{a_{A^- \cdot h_w H_2O} \cdot a_{C^+}}{a_{CA} \cdot \left(a_{H_2O}\right)^{h_w}} = \frac{x_{A^- \cdot h_w H_2O} \cdot x_{C^+}}{x_{CA} \cdot \left(x_{H_2O}\right)^{h_w}} \cdot \frac{\gamma_{A^- \cdot h_w H_2O} \cdot \gamma_{C^+}}{\gamma_{CA} \cdot \left(\gamma_{H_2O}\right)^{h_w}} \qquad (13)$$

Based on this strategy, there were four true species, *i.e.*, cations (C^+), ion-pair (CA), hydrated anion ($A^- \cdot h_w H_2O$), and H_2O. For the IL-H_2O binary systems with N_{H2O} apparent moles of water and N_{CA} apparent moles of water IL, according to this strategy, the number of moles of free water, free CA (n^f_{CA}) and free C^+ in this solution, is:

$$\begin{aligned} n^f_{H_2O} &= N_{H_2O} - h_w \cdot n^f_{A^- \cdot h_w H_2O} \\ n^f_{CA} &= N_{CA} - n^f_{A^- \cdot h_w H_2O} \\ n^f_{C^+} &= n^f_{A^- \cdot h_w H_2O} \end{aligned} \qquad (14\text{-}1)$$

The n_T for all the species is given by:

$$n_T = n^f_{H_2O} + n^f_{CA} + n_{C^+} + n^f_{A^- \cdot h_w H_2O} = N_{H_2O} + N_{CA} + \left(1 - h_w\right) \cdot n^f_{A^- \cdot h_w H_2O} \qquad (14\text{-}2)$$

Therefore, the true mole fraction of these species is given as follows:

$$\begin{aligned} x_{H_2O} &= n^f_{H_2O} / n_T \\ x_{CA} &= n^f_{CA} / n_T \\ x_{C^+} &= x_{A^- \cdot h_w H_2O} = n^f_{A^- \cdot h_w H_2O} / n_T \end{aligned} \qquad (14\text{-}3)$$

For the addition of the association equilibrium, the interaction between cation and anion was reflected by association equilibrium constant K_a. The interaction between CA and H_2O was reflected by adjustable parameters ($\tau_{m,m'}$ and $\tau_{m',m}$). The anion A^- was considered as fully hydrated. The interaction between all the ions and H_2O was neglected. Therefore, three groups of adjustable parameters, including two binary interaction parameters $\tau_{m,m'}$ and $\tau_{m',m}$, and one association equilibrium constant K_a.

3.3 Relationship between G^E and apparent properties. The thermodynamic model is to describe G^E, which is reflected in the excess properties. In this work, the excess properties related to the activity coefficients, i.e., osmotic coefficient and enthalpy of mixing in the IL-water system, were determined and used in modeling. For enthalpy of mixing H_m, according to the Gibbs-Helmholtz equation Eq. (15), the H_m is directly related to the temperature dependence of G^E. The symmetric expression of G^E in Eqs. (4) and (5) was used to obtain H_m in this work.

$$H_m = -RT^2\left(\frac{\partial\left(G^E/RT\right)}{\partial T}\right)_{P,x} = -RT^2\left(\frac{\partial\left(G^{E,SR}/RT\right)}{\partial T}+\frac{\partial\left(G^{E,LR}/RT\right)}{\partial T}\right)_{P,x} \quad (15)$$

The osmotic coefficient is related to the true activities of solutes and water in the system. The practical osmotic coefficient is defined as the measured osmotic pressure divided by the ideal osmotic pressure. The relation between the practical osmotic coefficient and the activity of solvent (a_s)[27] is:

$$\Phi^{(m)} = -1000\Phi^{(x)}\ln x_s/\left(\nu m_s M_s\right)$$
$$\Phi^{(x)} = \frac{\ln(a_s)}{\ln x_s} = \frac{\ln(x_s\times\gamma_s)}{\ln x_s} \quad (16)$$

where $\Phi^{(m)}$ is the molality osmotic coefficient; $\Phi^{(x)}$ is the rational osmotic coefficient; m_s is the molality of the solute, mol· kg^{-1}; a_s is the activity of the solvent; x_s is the true mole fraction of the solvent; γ_s is the activity coefficient of the solvent.

4. Results and discussion

4.1 Experimental results. *4.1.1 Enthalpy of mixing* H_m. The H_m of HmimCl/Br/I-H_2O systems over the entire compositional range at 298.15, 308.15 and 318.15 K under 0.1 MPa was reported in this work for the first time. The measured data are listed in Table 1 and illustrated in Error: Reference source not found. As we can see from Error: Reference source not found, the values of H_m were positive for the binary systems of HmimI-H_2O over the entire compositional range indicating an endothermic mixing. While for the HmimBr-H_2O binary system, the H_m showed 'S' shape, and the values changed from negative to positive with increasing the content of H_2O, meaning that the mixing process changed from exothermic to endothermic with the increase of water content. When the anion in IL changed to be Cl^-, the values of H_m became negative over the entire compositional range, that is, the mixing was exothermic. Considering that the only difference in these three binary systems is the size of the anion, therefore, the differences in the value and shape of H_m are closely related to the size of the anion. The crystal sizes of Cl^-, Br^- and I^- are listed in Table 2. The results indicated that for the studied systems, the values of H_m changed from positive to negative with the decrease of the size of anion, which meant that decreasing the size of the anion ($I^- > Br^- > Cl^-$) in IL made the mixing of IL with H_2O changed from endothermic to exothermic. The smaller size of the anion, the stronger the interaction force between cation and anion is (association or dissociation); meanwhile, the ionic size essentially determines the ionic hydration, *i.e.*, the smaller size, the stronger hydration. These dual effects led to the changes of the H_m for these three IL-H_2O mixing systems.

In addition, the operating temperature also affected the results of H_m. The value of H_m became more positive with increasing temperature for all the mixtures studied in this work. In other words, the curve of H_m against mole fraction of IL moved upwards when the temperature increased. It meant that with the increase of temperature, the heat absorbed from the outside

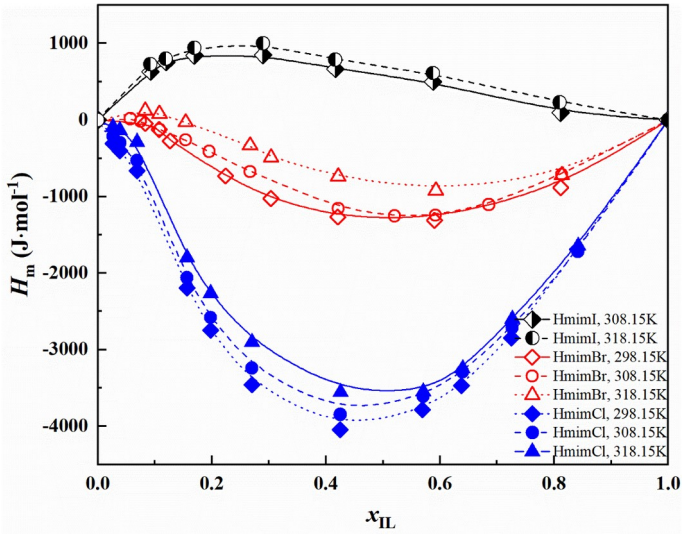

Fig. Molar enthalpy of mixing (H_m) of [H_2O (1)- HmimCl (2) or -HmimBr (2) or -HmimI (2)] at different temperatures. Lines: a guide of eyes.

system increased or heat liberated to the outside system decreased. The reason may because that the temperature increase resulted in the decreased dielectric constant and relative polarity of water, which weaken the bonding between water and IL (*i.e.*, hydration of IL).

Table 1 H_m of H_2O(1)- IL(2) at different temperatures and 0.1 MPa*

x_1	$10^3\times u(x_1)$	H_m/(J·mol^{-1})	u (H_m)	x_1	$10^3\times u(x_1)$	H_m/(J·mol^{-1})	u (H_m)
HmimCl(2)-H_2O(1) (298.15 K)				HmimCl(2)-H_2O(1) (308.15 K)			
0.1578	0.4454	-1688.28	12.47	0.1583	0.0930	-1718.89	7.47
0.2734	0.0754	-2843.57	5.34	0.2733	0.1156	-2714.65	11.65
0.3604	0.0913	-3466.66	14.37	0.3608	0.1073	-3288.78	13.67
0.4294	0.1786	-3784.84	21.64	0.4296	0.0855	-3609.23	12.95
0.5742	0.1377	-4047.15	13.90	0.5745	0.0023	-3848.59	19.95
0.7296	0.1264	-3458.43	15.46	0.7297	0.0133	-3240.83	1.29
0.8020	0.0726	-2745.36	12.17	0.8021	0.0159	-2579.6	5.22
0.8437	0.0833	-2192.77	16.55	0.8438	0.0166	-2059.31	4.31

0.9312	0.1132	-663.91	14.78	0.9311	0.0052	-531.55	4.03
0.9612	0.0399	-399.90	12.51	0.9612	0.0019	-298.22	2.97
0.9730	0.0231	-306.85	10.30	0.9730	0.0004	-214.18	3.17
HmimCl(2)-H_2O(1) (318.15 K)				HmimBr(2)-H_2O(1) (308.15 K)			
0.1592	0.0000	-1647.74	7.56	0.1865	0.0000	-715.18	11.89
0.2753	0.1803	-2599.64	18.10	0.3144	0.5525	-1105.21	6.91
0.3628	0.1441	-3247.5	12.30	0.4081	0.4186	-1265.11	5.46
0.4314	0.1386	-3551.34	14.63	0.4795	0.0786	-1254.14	7.79
0.5748	0.2361	-3557.46	31.71	0.5785	0.0491	-1196.63	6.45
0.7300	0.0600	-2903.13	28.72	0.7329	0.0237	-673.64	11.85
0.8021	0.1241	-2265.47	32.50	0.8046	0.0829	-412.00	6.14
0.8438	0.0527	-1799.35	32.67	0.8459	0.0247	-259.58	14.72
0.9309	0.0395	-290.55	5.07	0.8916	0.0018	-126.28	11.20
0.9611	0.0284	-135.5	1.93	0.9250	0.0600	-18.11	5.13
0.9730	0.0310	-92.73	0.90	0.9427	0.0037	16.48	6.07
HmimBr(2)-H_2O(1) (318.15 K)				HmimBr(2)-H_2O(1) (298.15 K)			
0.1862	0.0008	-721.83	19.61	0.1884	0.0001	-880.87	9.89
0.4073	0.2774	-924.77	13.60	0.4095	0.5525	-1310.02	11.91
0.5788	0.0584	-739.86	4.54	0.5791	0.4186	-1245.64	5.46
0.6960	0.1113	-489.20	6.16	0.6964	0.0786	-1026.41	7.79
0.7332	0.3719	-331.63	4.32	0.7755	0.0491	-731.88	4.45
0.8461	0.2630	-29.96	3.69	0.8733	0.0237	-274.51	9.85
0.8919	0.1082	80.12	6.16	0.8924	0.0829	-124.06	5.14
0.9166	0.6458	119.62	4.23				
HmimI(2)-H_2O(1) (308.15 K)				HmimI(2)-H_2O(1) (318.15 K)			
0.1887	0.7868	109.31	5.79	0.1898	0.2144	224.48	6.39
0.4122	0.2991	493.59	4.99	0.4122	0.0002	640.35	11.31
0.5836	0.3222	668.53	12.68	0.5836	0.1320	841.07	8.02
0.7101	0.0457	890.14	8.35	0.7103	0.1865	1006.19	13.41
0.8305	0.0234	847.80	4.63	0.8306	0.0036	935.57	7.54
0.8803	0.0750	745.83	9.29	0.8803	0.0191	821.41	9.55
0.9075	0.0728	654.98	7.95	0.9074	0.0217	718.45	3.79

*x_1 is the apparent mole fraction of H_2O in the mixture of IL and H_2O. x_2 is the apparent mole fraction of IL in the mixture of IL and H_2O. $x_2 = 1 - x_1$. The abbreviation u(i) is used for the standard uncertainty of quantity i: u(T) = 0.02 K, u(P) = 3 kPa. H_m is the molar enthalpy of mixing in Joule per mol mixture.

Table 2 Crystal sizes (diameters, σ_a) of anions[27] used in this work

Ions	σ_a / Å
Cl^-	3.62
Br^-	3.92
I^-	4.32

4.1.2 Electrical conductivity Λ. The *Λ* of HmimCl/Br/I – H_2O over the entire compositional range at 303.2 K was reported. The results are shown in and Error: Reference source not found. As we can see in Error: Reference source not found, the *Λ* increased sharply to a maximum point then decreased to less than 1 $mS \cdot cm^{-1}$ with the increase of IL content. The maximum value of *Λ* for these three ILs with water followed the trend: HmimCl > HmimBr > HmimI. According to the Onsager theory, the molar electrical conductivity falls with the square root of the ion concentration.[28] The results showed that with the same water content (mole fraction of water), the HmimCl-H_2O system had the highest ion concentration, followed by HmimBr-H_2O and HmimI-H_2O systems. It implied that more free ions existed in the infinite diluted solution of HmimCl. The only difference for all these ILs is the size of anion, and thus, the hydration degree of ions and the dissociation degree of IL caused by the size of anion may be the main reason for the difference of *Λ*. The position of an extreme point (maximum *Λ*) for these ILs-H_2O systems was around x_{IL}=0.05, and the position slightly moved toward the IL-rich direction with the increase of the size of the anion. When $0.4>x_{IL}>0.05$, the *Λ* decreased dramatically. Afterward, the *Λ* changed slightly to the value of pure IL. The size of ions had little effect on the trend of the *Λ* against the mole fraction of IL.

Table 3 *Λ* of H_2O(1)-IL(2) at 303.2 K*

HmimCl(2)-H_2O(1)		HmimBr(2)-H_2O(1)		HmimI(2)-H_2O(1)	
x_1	$\Lambda/(mS \cdot cm^{-1})$	x_1	$\Lambda/(mS \cdot cm^{-1})$	x_1	$\Lambda/(mS \cdot cm^{-1})$
0.990	29.090	0.990	28.340	0.990	23.790
0.980	43.230	0.978	41.170	0.980	30.680
0.960	54.240	0.960	48.400	0.970	35.690
0.940	55.390	0.940	49.690	0.950	38.300
0.920	51.720	0.920	47.830	0.930	38.270
0.900	47.120	0.900	43.360	0.915	36.280
0.800	22.810	0.799	23.190	0.826	23.920
0.698	10.350	0.657	8.487	0.733	13.310

0.568	4.507	0.553	3.954	0.642	8.291
0.491	1.841	0.450	1.846	0.538	4.739
0.399	0.892	0.346	0.887	0.427	2.445
0.283	0.362	0.245	0.454	0.319	1.314
0.179	0.192	0.147	0.221	0.205	0.728
0.083	0.138	0.052	0.153	0.078	0.364

*The abbreviation u(i) is used for the standard uncertainty of quantity i: u(T) = 0.5 K, u(Λ) = 0.05 mS·cm^{-1}, u(x)= 0.003.

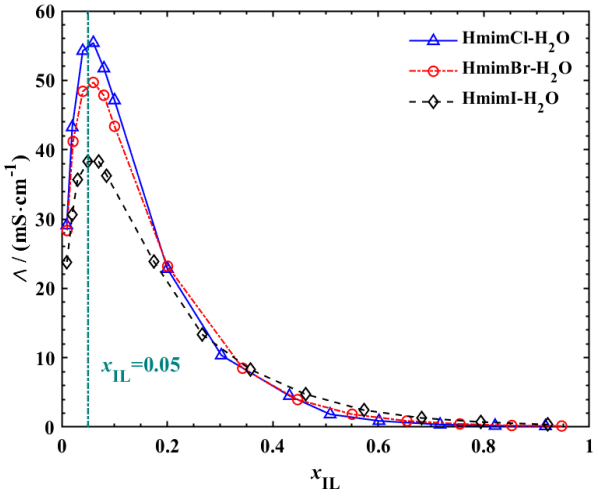

Fig. Electrical conductivity (Λ) of [H_2O(1)-HmimCl(2) or -HmimBr(2) or -HmimI(2)] at 303.2 K. Lines: a guide of eyes.

4.2 Modeling results. *4.2.1. Comparison.* The experimental values of H_m measured in this work and Φ reported in the literature (summarized in Table 4) were used simultaneously to obtain the fitting parameters in different models. The other required model parameters needed in the eNRTL model were fixed and summarised in Table 5. It should be mentioned that when IL ion-pair existed in the system (strategy 2), IL was considered as another solvent besides water. Therefore, the dielectric constant of these ILs was considered, and the values reported by Rybinska-Fryca *et al.*[29] (Table 5) were adopted in this work. The temperature effect on the

dielectric constant of these ILs was not considered. For the mixed solvents, mixing rules[17] for the solvent molecular weight M_i and dielectric constant D_i are expressed in Eq. (17):

$$M_s = \sum_i x_i M_i$$
$$D_s = \sum_i \left(\frac{x_i M_i}{\sum_j x_j M_j} \right) D_i \qquad (17)$$

Table 4 Osmotic coefficient $\Phi^{(m)}$ of H_2O(1)-Hmim X (X = Cl, Br) (2)

	*M*olality m_2/ mol·kg^{-1}	*T*/K	Number of data points	Ref.
HmimCl(2)-H_2O(1)	0.0932-4.1289	313.15, 333.15	34	**30**
	0.1399-3.9318	298.15	34	**31**
	0.0248-0.869	308.15	15	**32**
HmimBr(2)-H_2O(1)	0.0155-2.3976	298.15-328.15	76	**33**

Table 5 Model parameters for eNRTL model

Born Radius of ionic species[34]		Dielectric Constant of Solvents D_i^*		
Ionic species	Born radius (Å)	Solvent *i*	d_1	d_2
Cl^-	1.81	Water	1.94315	0.001972
Br^-	1.96	HmimCl	11.75[29]	—
I^-	2.16	HmimBr	11.75[29]	—
$[Hmim]^+$	—	HmimI	11.75[29]	—

*$logD_i=d_1-d_2(T-273.15)$, *T* is the system temperature, K.

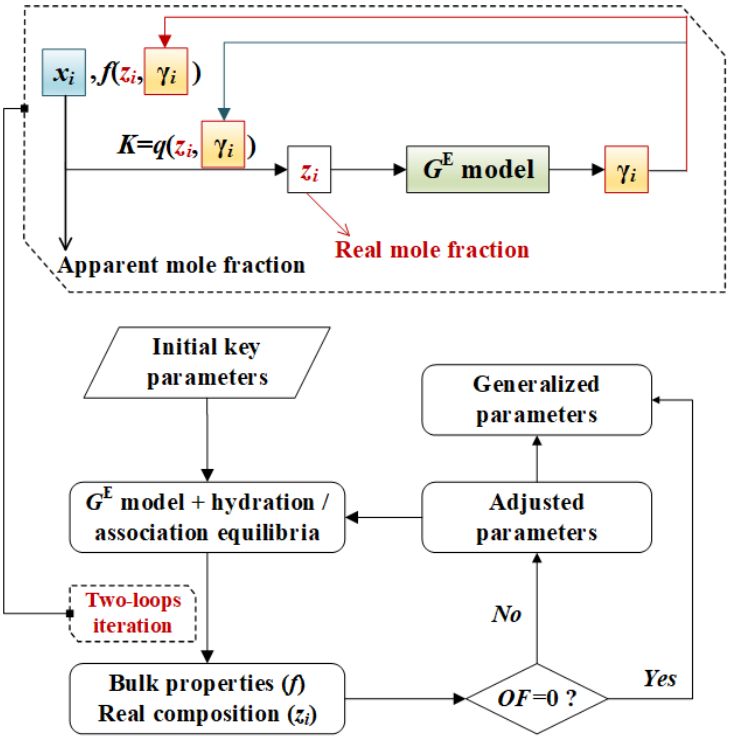

Fig. 3 Model parameterizing process

A two-loop iteration is used to correlate the thermodynamic properties related to activity coefficient γ_i and the composition z_i of real species (cation, anion, hydrated anion, ion-pair or H_2O). The experimental values of H_m and $\Phi^{(m)}$ were fitted simultaneously, and the objective function (OF) defined in Eq. (18) was used for minimization to obtain the fitting parameters for all the models. The model parameterizing process was depicted in Fig. 3.

$$OF = \left| \left(\frac{H_m^{exp} - H_m^{cal}}{H_m^{exp}} \right) \right| + \left| \frac{\left(\Phi^{exp} - \Phi^{cal} \right)}{\Phi^{exp}} \right| \quad (18)$$

For the NRTL model, the fitting parameters in Eq. (2) are listed in Table 6, together with ARD. As we can see from Table 6, adding c_{ij} as another adjustable parameter can slightly improve the performance for HmimCl-H_2O and HmimI-H_2O systems while greatly

improved the performance from *ARD* 54.84 to 47.11 % for the HmimBr-H_2O system. For the HmimI-H_2O system, only H_m data is available, and using NRTL can represent this property well (*ARD* <10.6 %). Considering that IL may exist as ions and ion-pairs, the model NRTL cannot reflect the distribution of the real species in these systems.

The eNRTL models, based on two different strategies, were also used to fit the experimental values of H_m and $\Phi^{(m)}$. The nonrandomness factor c was set to 0.2 during modeling. The objective function *OF* shown in Eq. (18) for minimization was used. The *ARD* and the adjustable parameters for different modeling strategies are listed in Table 7.

Table 6 Parameters of NRTL equation with *ARD* for H_2O(1)-IL(2)*

H_2O(1)-IL(2)	$10^{-3}\times\triangle g_{ij\,(H2O,\,IL)}$	$10^{-3}\times\triangle g_{ij\,(IL,\,H2O)}$	c_{ij}	*ARD* of H_m, %	*ARD* of $\phi^{(m)}$, %	*ARD*, %
H_2O(1)-HmimCl(2)	15.91	-7.52	0.2	26.90	6.22	14.34
	38.67	-22.81	0.04	20.53	7.98	12.90
H_2O(1)-HmimBr(2)	10.79	-4.56	0.2	53.08	55.46	54.84
	67.81	-46.19	0.01	39.61	49.77	47.11
H_2O(1)-HmimI(2)	11.40	-0.20	0.2	10.54	—	—
	13.78	-3.27	0.11	10.05	—	—

**Absolute Average Relative Deviation,* $ARD = \left(\sum_{i=1}^{NP} \left| \left(f_i^{exp} - f_i^{cal} \right) / f_i^{exp} \right| \right) \cdot (1/NP)$, $\tau_{ij}=\triangle g_{ij}/RT$

Table 7 Parameters of eNRTL model with *ARD* for H_2O(1)-IL(2)*

eNRTL						
H_2O(1)-IL(2)	$10^{-3}\times(\triangle g_{mc,ac}=\triangle g_{ma,ca})$	$10^{-3}\times(\triangle g_{cm}=\triangle g_{am})$	*ARD*, %			
			H_m	$\Phi^{(m)}$	*total*	
H_2O(1)-HmimCl(2)	17.26	-7.41	34.65	6.5	14.79	
H_2O(1)-HmimBr(2)	14.09	-5.76	56.87	38.34	43.19	
H_2O(1)-HmimI(2)	8.38	-2.80	8.52	—	—	
eNRTL$_{SI}$						
H_2O(1)-IL(2)	$10^{-3}\times(\triangle g_{mc,ac}=\triangle g_{ma,ca})$	$10^{-3}\times(\triangle g_{cm}=\triangle g_{am})$	A_1 (in lnK_h)	A_2 (in lnK_h)	*ARD*, %	
					H_m	$\Phi^{(m)}$	*total*
H_2O(1)- h_w=2	17.08	-7.40	-1.22	-6027.9	35.30	5.68	14.41

HmimCl(2)	h_w=4	17.17	-7.42	2.67	-6569.0	35.04	5.88	14.47
	h_w=6	17.10	-7.41	1.80	-6517.6	35.28	5.63	14.37
H_2O(1)-HmimBr(2)	h_w=2	13.14	-5.72	-74.7	5756.2	43.41	41.81	42.23
	h_w=4	13.12	-5.73	-132.1	5842.8	42.92	41.94	42.20
	h_w=6	13.02	-5.71	-193.2	5836.8	42.68	42.24	42.35
H_2O(1)-HmimI(2)	h_w=2	8.41	-2.80	-19.0	2219.2	8.58	—	—
	h_w=4	8.41	-2.80	-20.0	2588.3	8.57	—	—
	h_w=6	8.40	-2.81	-20.9	2094.7	8.54	—	—

eNRTL$_{S2}$

H_2O(1)-IL(2)		$10^{-3}\times\triangle g_{mm'}$	$10^{-3}\times\triangle g_{m'm}$	B_1 (in lnK_a)	B_2 (in lnK_a)	*ARD*, %		
						H_m	$\Phi^{(m)}$	*total*
H_2O(1)-HmimCl(2)	h_w=0	16.19	-7.31	139.54	-48887.2	29.69	64.82	13.32
	h_w=2	16.61	-7.64	62.84	-22935.4	26.39	6.24	12.18
	h_w=4	17.74	-8.58	20.16	-8176.5	20.18	5.91	10.12
	h_w=6	17.75	-8.94	7.38	-3691.0	15.35	5.00	8.05
H_2O(1)-HmimBr(2)	h_w=0	15.12	-5.13	128.8	-44398.6	39.69	40.90	40.58
	h_w=2	15.31	-5.18	110.2	-38355.1	33.63	39.87	38.24
	h_w=4	15.22	-5.18	114.1	-39523.9	33.67	40.10	38.41
	h_w=6	15.14	-5.17	122.7	-42204.1	33.81	40.32	38.61
H_2O(1)-HmimI(2)	h_w=0	11.40	-0.20	14.1	-9535.29	6.57	—	—
	h_w=2	11.40	-0.26	2.11	-5742.48	7.56	—	—
	h_w=4	11.45	-0.22	3.87	-6125.67	7.40	—	—
	h_w=6	11.22	-0.25	2.28	-5991.36	8.17	—	—

* $\tau_{jc,ac}=\triangle g_{jc,ac}/RT$; $\tau_{ja,ca}=\triangle g_{ja,ca}/RT$; $\ln K_h=A_1+A_2/T$; $\ln K_a=B_1+B_2/T$.

As we can see from Table 6 and Table 7, the comparison of the model performance (*i.e.*, *ARD*) of the H_m and $\Phi^{(m)}$ for these binary systems shows that NRTL and original eNRTL model give the similar model performance (similar *ARD*) for H_2O-HmimCl system, while for the other systems, eNRTL model provides smaller *ARD* in describing these two properties together. This implies that an ion-based model should be used for describing the nonideality of these systems over the whole compositional range. The eNRTL model adding hydration equilibrium (eNRTL$_{S1}$) slightly increased the model performance than the original eNRTL model (*ARD:* decreased from 14.79% to 14.37% for the H_2O-HmimCl system and changed from 43.19% to 42.20% for the H_2O-HmimBr system). The eNRTL model with strategy 2 (eNRTL$_{S2}$) significantly improved the model performance, e.g., *ARD* decreased from 14.79% to 8.05% for H_2O- HmimCl system, and a

larger hydration number resulted in a smaller *ARD*. This implies that the consideration of IL association or dissociation is necessary.

In addition, to investigate how the hydration number influences the model performance, the models (eNRTL$_{S1}$ and eNRTL$_{S2}$) with different hydration numbers, *i.e.*, 2, 4, and 6 were studied to model these three systems and the results are shown in Table 7 and Error: Reference source not found. It showed that the increased hydration number slightly affected the model performance of the eNRTL$_{S1}$ model, i.e., *ARD* decreased from 14.54% to 14.37% when the hydration number changed from 2 to 6. It means that the effect of hydration number on eNRTL$_{S1}$ model can be ignored in representing these two properties over the entire compositional range. The effect of the hydration number on the model performance of eNRTL$_{S2}$ model was more significant than that in eNRTL$_{S1}$ model, but for different systems, the influence of the hydration number was varied. For H_2O-HmimCl system, setting hydration number as 6 significantly improved the performance from *ARD* 12.18% from 8.05% while the hydration number slightly affected the performance of H_2O-HmimBr. For H_2O-HmimI system, the smaller hydration

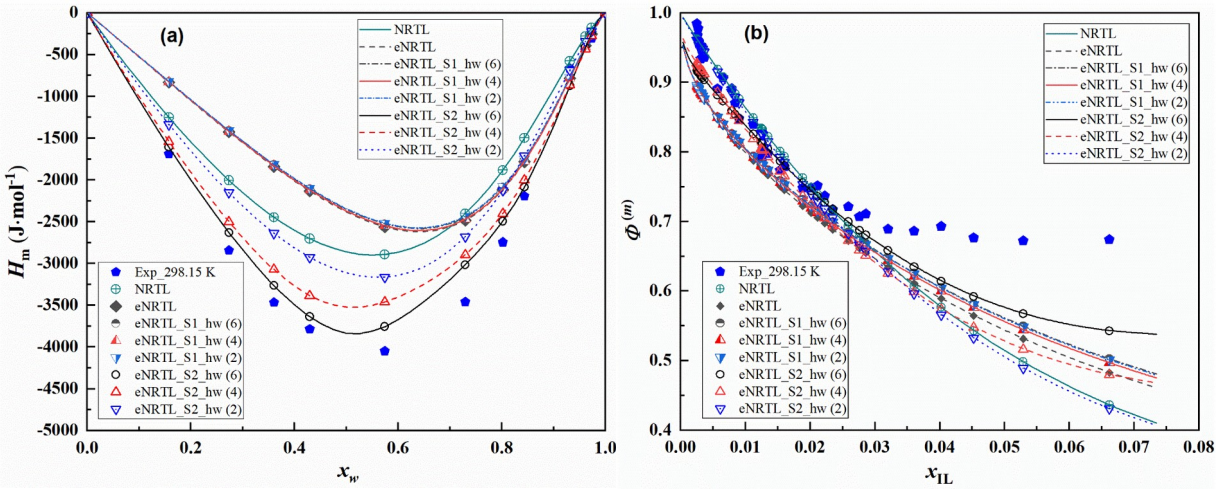

Fig. Comparison of experimental results and model results for H_2O -HmimCl at 298.15 K. (a). Enthalpy of mixing H_m; (b).Osmotic coefficient $\Phi^{(m)}$. Curves: model predicted results. x_w and x_{IL} are apparent mole fraction of water and IL, respectively.

number is recommended. In $eNRTL_{S2}$ model, when the hydration number is 0, it means that only IL association or dissociation was considered. By comparison model performance of different models, it showed that including IL association or dissociation was of great importance to well representing the properties. For H_2O- HmimI system, only considering IL association or dissociation is enough to get small *ARD*. Considering only anions are different in these three systems, it implies that the hydration and hydration number rely on the size of the anion. For H_2O-HmimBr and H_2O-HmimI systems, available osmotic coefficient data from literature is limited. Therefore, to finally confirm the hydration number, the molecular simulation and experimental study in the IL diluted region should be investigated in the future.

Error: Reference source not found shows the comparison of the experimental results and model results for H_2O- HmimCl system. The enthalpy of mixing using eNRTL model of strategy 2 (with dissociation equilibrium and fully hydration) setting hydration number to be 6 agreed best with the experimental data. The comparison of the deviation between the modeling results and experimental data of H_m in the IL diluted region ($0<x_{IL}<0.5$) and that in the IL rich region ($0.5<x_{IL}<1$) showed that NRTL model gave the largest deviation in IL diluted region, while it showed small error in IL rich region. This result meant that when the IL-H_2O system is rich with IL, the molecular model can still be used to describe the system.

4.2.2. Further analyses using the eNRTL model with new strategies. Based on the paraments listed in Table 7 and the equations in section 3, the composition of all species and true ionic strength based on mole fraction and molarity (I_x and I_m) can be obtained. In this section, H_2O-HmimCl system was selected to further investigate. For the $eNRTL_{S2}$ model, the degree of

dissociation α_d and association α_a of IL can be predicted, and the definition of α_d and α_a of IL are presented in the following equation:

$$\alpha_a = 1 - \alpha_d = 1 - \frac{n^f_{C^+}}{n^f_{C^+} + n^f_{CA}} = \frac{n^f_{CA}}{n^f_{C^+} + n^f_{CA}} \quad (19)$$

Herein, Error: Reference source not founda depicts the ionic strength based on mole fraction I_x and degree of association α_a with different apparent water content x_w based on different models and hydration numbers. As we can see from Error: Reference source not founda, using the eNRTL$_{S1}$ model, the total I_x decreased with the increase of water content x_w continuously. While when using the eNRTL$_{S2}$ model, the highest I_x occurred at $x_w \approx$ 0.8-0.9 ($x_{IL} \approx$ 0.1-0.2). The degree of association α_a for H_2O-HmimCl system at 298.15 K changing with apparent water content is also shown in Error: Reference source not founda. The hydration number affects the association degree greatly. When the hydration number is 2, the dissociation was negligible. According to the previous modeling results, setting the hydration number to be 6 agreed best with the experimental data for H_2O- HmimCl system. In this hydration number, when x_w was larger than 0.4, IL started to be dissociated. When x_w was close to 1, that is, IL infinite dilution, the degree of dissociation α_d of IL reached 100%, which meant that IL existed as ions at this status. This result brought to light how water alters the microstructure in ILs quantitatively and how to control the water content to keep more IL ion-pairs. However, for other systems, more properties such as osmotic coefficient and vapor pressure are needed to be measured in the future to get more accurate model prediction results.

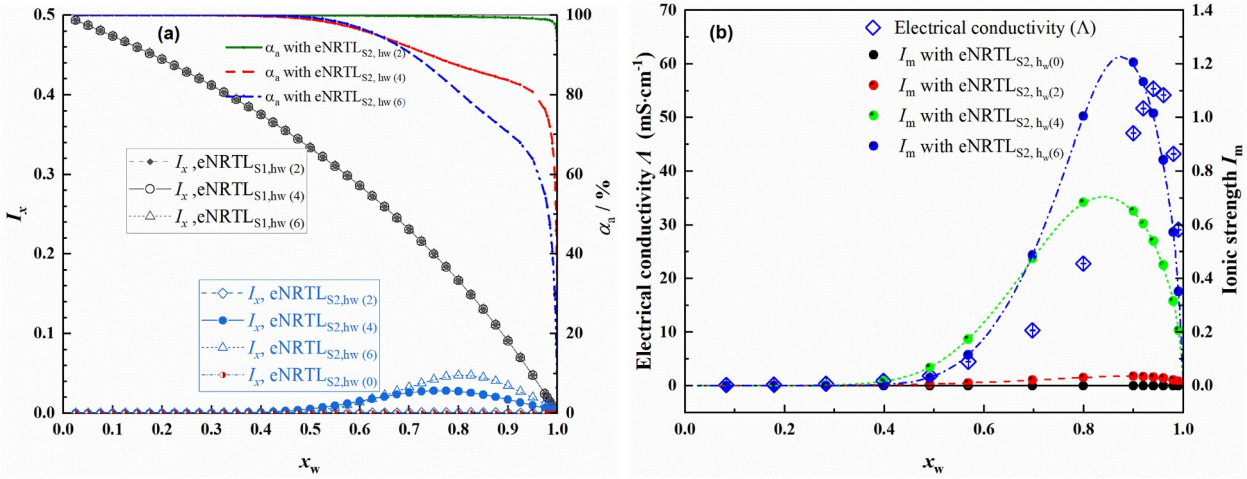

Fig. (a) The ionic strength based on mole fraction and degree of association α_a for H_2O-HmimCl with different water content using different models with different h_w at 298.15 K; (b) the true ionic strength based on molarity I_m at 303.15 K using eNRTL$_{S2}$ model with different h_w and the corresponding the electrical conductivity measured in this work. x_w is the apparent mole fraction of water.

As discussed in section 4.1.2, the position of the extreme point of the electrical conductivity Λ for the H_2O- HmimCl system was around $x_{IL}\approx0.05$. Error: Reference source not foundb shows the true ionic strength based on molarity I_m at 303.15 K using the eNRTL$_{S2}$ model with different hydration numbers. The extreme point of I_m occurred $x_{IL}\approx$ 0.1-0.2. With the increase of hydration number, the value of the extreme point of I_m increased, and the position of the extreme point moved towards a more diluted IL solution. Obviously, the electrical conductivity Λ is closely related to I_m, especially when the hydration number is 6. Error: Reference source not found shows the link between the true I_m using the eNRTL$_{S2}$ model by setting h_w as 6 and the Λ for H_2O- HmimCl system. When $0<x_w<0.9$, the electrical conductivity Λ is linearly related (coefficient of determination R^2: 0.989) with true I_m. While when in the region $0.9<x_w<1$, there is polynomial relation (R^2: 0.997) between Λ and true I_m. The turning point x_w=0.9 is the position of the extreme point of I_m. This correlation between Λ and true I_m gives the possibility of quantitatively predicting the electrical conductivity from other macro properties.

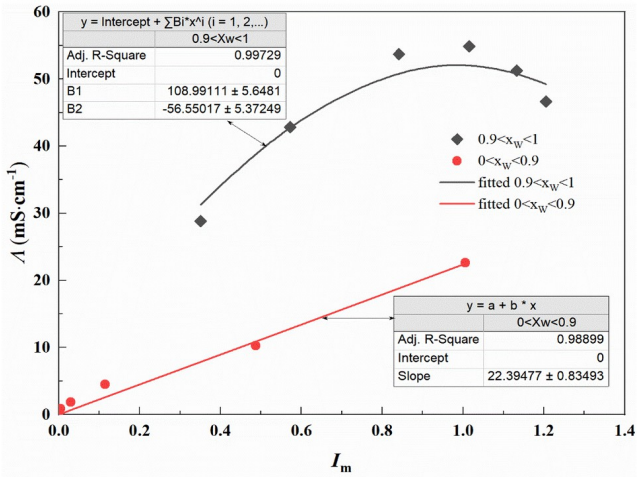

Fig. The correlation between the true I_m using eNRTL$_{S2}$ model (h_w=6) and the electrical conductivity for H_2O (1) + HmimCl (2)

5. Conclusion

The NRTL model, original eNRTL model, and eNRTL model including new strategies (hydration or association) were investigated to model the IL- H_2O systems' enthalpy of mixing and osmotic coefficient altogether. Three typical IL- H_2O systems with the same cation, *i.e.*, $[Hmim]^+$ but the different size of anions, *i.e.*, Cl^-, Br^-, and I^- were selected to conduct modeling. The data of the enthalpy of mixing used in this work was measured and reported for the first time. The model performance was compared, and the model with new strategies was further analyzed. The electrical conductivity of these systems over the entire compositional range was also measured for further comparison with model prediction results. The experimental results of the enthalpy of mixing showed that decreasing the size of the anion (I^-> Br^- >Cl^-) in IL made the mixing of IL with H_2O changed from endothermic to exothermic. The electrical conductivity of these IL-H_2O systems showed a maximum point over the entire compositional range, whose

position was around x_{IL}=0.05, and it slightly moved toward the IL-rich region with increasing the size of the anion.

The modeling results show that the ion-based eNRTL model showed a smaller *ARD* compared with the molecule-based NRTL model. The eNRTL model adding hydration equilibrium only slightly increased the model performance (*ARD* slightly decreased) than the original eNRTL model. The eNRTL model with association equilibrium and hydration showed the best performance (smallest *ARD*) among all models studied in this work for all these IL-H_2O systems. The hydration number affected its model performance, and its influence depends on the halide anion. Further analyses show that for the H_2O-HmimCl system, when x_w is larger than 0.4, IL started to be dissociated. When it is at IL infinite dilution, the degree of dissociation of IL can reach 100%. The predicted real ionic strength I_m presents an extreme point at a similar position to the maximum of the electrical conductivity. Two regimes ($0.9<x_w<1$ and $0<x_w<0.9$) of the correlation between I_m and electrical conductivity were observed, and the turning point shows on the position of the extreme point of I_m. This result gives the possibility of quantitatively predicting the electrical conductivity from other macro properties such as enthalpy of mixing. In future work, more properties are needed to be measured, especially osmotic coefficient, and the models including dissociation and hydration equilibria are needed to be investigated.

Acknowledgment

This work was supported by the Swedish Research Council (2020-03899), the Joint Research Fund for Overseas Chinese Scholars and Scholars in Hong Kong and Macao Young Scholars (No. 21729601), and the National Natural Science Foundation of China (No. 21838004).

Reference

1. Rogers RD, Seddon KR. Ionic Liquids--Solvents of the Future? 2003;302(5646):792-793.

2. Ramdin M, de Loos TW, Vlugt TJH. State-of-the-Art of CO2 Capture with Ionic Liquids. Industrial & Engineering Chemistry Research. 2012/06/20 2012;51(24):8149-8177.

3. Zhou Y, Qu J. Ionic Liquids as Lubricant Additives: A Review. ACS Applied Materials & Interfaces. 2017/02/01 2017;9(4):3209-3222.

4. Swatloski RP, Spear SK, Holbrey JD, Rogers RD. Dissolution of Cellose with Ionic Liquids. Journal of the American Chemical Society. 2002/05/01 2002;124(18):4974-4975.

5. Wasserscheid P, Keim W. Ionic Liquids—New "Solutions" for Transition Metal Catalysis. Angew. Chem. Int. Ed. . 2000;39(21):3772-3789.

6. Fendt S, Padmanabhan S, Blanch HW, Prausnitz JM. Viscosities of Acetate or Chloride-Based Ionic Liquids and Some of Their Mixtures with Water or Other Common Solvents. Journal of Chemical and Engineering Data. Jan 2011;56(1):31-34.

7. Malham IB, Turmine M. Viscosities and refractive indices of binary mixtures of 1-butyl-3-methylimidazolium tetrafluoroborate and 1-butyl-2,3-dimethylimidazolium tetrafluoroborate with water at 298 K. Journal of Chemical Thermodynamics. Apr 2008;40(4):718-723.

8. Widegren JA, Magee JW. Density, viscosity, speed of sound, and electrolytic conductivity for the ionic liquid 1-hexyl-3-methylimidazolium bis(trifluoromethylsulfonyl)imide and its mixtures with water. Journal of Chemical and Engineering Data. Nov-Dec 2007;52(6):2331-2338.

9. Xie Y, Dong H, Zhang S, Lu X, Ji X. Effect of Water on the Density, Viscosity, and CO2 Solubility in Choline Chloride/Urea. Journal of Chemical & Engineering Data. 2014;59(11):3344-3352.

10. Torrecilla JS, Rafione T, Garcia J, Rodriguez F. Effect of relative humidity of air on density, apparent molar volume, viscosity, surface tension, and water content of 1-ethyl-3-methylimidazolium ethylsulfate ionic liquid. Journal of Chemical and Engineering Data. Apr 2008;53(4):923-928.

11. He Z, Zhao Z, Zhang X, Feng H. Thermodynamic properties of new heat pump working pairs: 1,3-Dimethylimidazolium dimethylphosphate and water, ethanol and methanol. Fluid Phase Equilibria. 11/15/ 2010;298(1):83-91.

12. Ma C, Shukla SK, Samikannu R, Mikkola J-P, Ji X. CO2 Separation by a Series of Aqueous Morpholinium-Based Ionic Liquids with Acetate Anions. ACS Sustainable Chemistry & Engineering. 2020/01/13 2020;8(1):415-426.

13. Li J, He C, Peng C, Liu H, Hu Y, Paricaud P. Modeling of the Thermodynamic Properties of Aqueous Ionic Liquid Solutions with an Equation of State for Square-Well Chain Fluid with Variable Range. Industrial & Engineering Chemistry Research. 2011/06/01 2011;50(11):7027-7040.

14. Mahato S, Kumar A, Banerjee T. PC-SAFT predictions on mixtures of 1-alkyl-3methylimidazolium-bis(trifluromethanesulphonyl)amide with hydrocarbons, alcohols and aqueous systems using a correlative based binary interaction parameter. Journal of the Taiwan Institute of Chemical Engineers. 2// 2016;59:69-78.

15. Tsioptsias C, Tsivintzelis I, Panayiotou C. Equation-of-state modeling of mixtures with ionic liquids. Physical Chemistry Chemical Physics. 2010;12(18):4843-4851.

16. Simoni LD, Ficke LE, Lambert CA, Stadtherr MA, Brennecke JF. Measurement and Prediction of Vapor−Liquid Equilibrium of Aqueous 1-Ethyl-3-methylimidazolium-Based Ionic Liquid Systems. Industrial & Engineering Chemistry Research. 2010/04/21 2010;49(8):3893-3901.

17. Simoni LD, Lin Y, Brennecke JF, Stadtherr MA. Modeling Liquid−Liquid Equilibrium of Ionic Liquid Systems with NRTL, Electrolyte-NRTL, and UNIQUAC. Industrial & Engineering Chemistry Research. 2008/01/01 2008;47(1):256-272.

18. Lin Y-J, Hossain N, Chen C-C. Modeling dissociation of ionic liquids with electrolyte NRTL model. Journal of Molecular Liquids. 2021/01/30/ 2021:115524.

19. Ma C, Laaksonen A, Liu C, Lu X, Ji X. The peculiar effect of water on ionic liquids and deep eutectic solvents. Chemical Society Reviews. 2018;47(23):8685-8720.

20. Sadeghi R, Ebrahimi N. Ionic Association and Solvation of the Ionic Liquid 1-Hexyl-3-methylimidazolium Chloride in Molecular Solvents Revealed by Vapor Pressure Osmometry, Conductometry, Volumetry, and Acoustic Measurements. The Journal of Physical Chemistry B. 2011/11/17 2011;115(45):13227-13240.

21. Renon H, Prausnitz JM. Local compositions in thermodynamic excess functions for liquid mixtures. AIChE Journal. 1968;14(1):135-144.

22. Chen C-C, Britt HI, Boston JF, Evans LB. Local composition model for excess Gibbs energy of electrolyte systems. Part I: Single solvent, single completely dissociated electrolyte systems. AIChE Journal. 1982;28(4):588-596.

23. Bollas GM, Chen CC, Barton PI. Refined electrolyte-NRTL model: Activity coefficient expressions for application to multi-electrolyte systems. AIChE Journal. 2008;54(6):1608-1624.

24. Pitzer KS, Simonson JM. Thermodynamics of multicomponent, miscible, ionic systems: theory and equations. The Journal of Physical Chemistry. 1986/06/01 1986;90(13):3005-3009.

25. Chen C-C, Bokis CP, Mathias P. Segment-based excess Gibbs energy model for aqueous organic electrolytes. AIChE Journal. 2001;47(11):2593-2602.

26. Nordness O, Brennecke JF. Ion Dissociation in Ionic Liquids and Ionic Liquid Solutions. Chemical Reviews. 2020/12/09 2020;120(23):12873-12902.

27. Kalyuzhnyi YV, Vlachy V, Dill KA. Aqueous alkali halide solutions: can osmotic coefficients be explained on the basis of the ionic sizes alone? Physical Chemistry Chemical Physics. 2010;12(23):6260-6266.

28. Zoski CG. Handbook of electrochemistry: Elsevier; 2006.

29. Rybinska-Fryca A, Sosnowska A, Puzyn T. Prediction of dielectric constant of ionic liquids. Journal of Molecular Liquids. 2018/06/15/ 2018;260:57-64.

30. González B, Calvar N, Domínguez Á, Macedo EA. Osmotic coefficients of aqueous solutions of four ionic liquids at T=(313.15 and 333.15) K. The Journal of Chemical Thermodynamics. 2008/09/01/ 2008;40(9):1346-1351.

31. Sadeghi R, Mahdavi A. (Vapour+liquid) equilibria, volumetric and compressibility behaviour of binary and ternary aqueous solutions of 1-hexyl-3-methylimidazolium chloride, methyl potassium malonate, and ethyl potassium malonate. The Journal of Chemical Thermodynamics. 2012/04/01/ 2012;47:347-357.

32. Sadeghi R, Ebrahimi N, Mahdavi A. Thermodynamic studies of the ionic liquid 1-hexyl-3-methylimidazolium chloride [C6mim][Cl] in polyethylene glycol aqueous solutions. The Journal of Chemical Thermodynamics. 2012/04/01/ 2012;47:48-55.

33. Shekaari H, Mousavi SS. Influence of alkyl chain on the thermodynamic properties of aqueous solutions of ionic liquids 1-alkyl-3-methylimidazolium bromide at different temperatures. The Journal of Chemical Thermodynamics. 2009/01/01/ 2009;41(1):90-96.

34. Chen C-C, Mathias PM, Orbey H. Use of hydration and dissociation chemistries with the electrolyte–NRTL model. AIChE Journal. 1999;45(7):1576-1586.